Electronic, Magnetic and Thermal Properties of Graphene-Diamond Hybrid Structure

T. Shiga,[1] S. Konabe,[2,3] J. Shiomi,[1,4] T. Yamamoto,[5] S. Maruyama,[1] and S. Okada[2,3,a)]

[1)] *Department of Mechanical Engineering, The University of Tokyo, Bunkyo-ku, Tokyo 113-8656, Japan*

[2)] *Graduate School of Pure and Applied Sciences, University of Tsukuba, Tsukuba, Ibaraki 305-8571, Japan*

[3)] *Japan Science and Technology Agency, CREST, Chiyoda, Tokyo 102-0075, Japan*

[4)] *Japan Science and Technology Agency, PRESTO, Kawaguchi, Saitama 332-0012, Japan*

[5)] *Department of Liberal Arts, Faculty of Engineering, Tokyo University of Science, Chiyoda-ku, Tokyo 102-0073, Japan*

(Dated: 8 March 2012)

We have theoretically investigated electronic, magnetic and thermal properties of a graphene-diamod hybrid structure consisting of a graphene nanoribbon with zigzag edges connected to diamond surfaces. Our first-principles electronic-structure calculations show that the graphene nanoribbon sandwiched in between diamonds serves as a spin-polarized conducting wire in the nano-scale electronic device circuits. Furthermore, by performing the non-equilibrium molecular dynamics simulations, it is demonstrated that the heat generated in the graphene nanoribbon can efficiently dissipate to the diamond region.

PACS numbers: 73.22.Pr, 85.75.-d, 65.80.Ck
Keywords: graphene, electronic structure, spin polarized transport, thermal transport

Current semiconductor technology is urging a miniaturization of electronic devices to advance integrability of devices along with advancing the switching speed and decreasing the power consumption[1]. To achieve the ultimate goal, it is necessary to explore the possibility of exotic materials with nanometer scale not only for conducting channel of metal-oxide-semiconductor field effect transistor (MOSFET) but also for conducting nanowire connecting the switching devices. In principle, the materials with high carrier mobility are plausible candidates for constituent materials for such electronic devices in the next generation. However, at the same time, increase of degree of integration of high-bias devices in circuits arise the problem that each device generates immense heat. Therefore, there is an additional requirement for the constituent materials of the devices in the post silicon era, which is to possess heat conduction channels for efficient thermal dissipation.

Carbon is one of possible elements for designing high-speed and low-heat devices in highly integrated circuits because it has a number of allotropes with various size and dimensionality in ranging from nano-meter size with zero/one dimension to bulk size with two/three dimension. Indeed, graphene exhibits remarkable carrier mobility up to 200,000 cm^2/Vs due to its unusual electronic structure around the Fermi level[2–5]. Further, the graphene, and carbon nanotubes are known to possess the highest thermal conductivity of any bulk material[6–11]. These facts indicate that the hybrid structures comprising of various carbon allotropes are promising candidates for the high-performance electronic devices, with a potential to replace the materials used in the current technology.

In the present work, we demonstrate a device structure for a conducting nanowire with a role of the heat sink by solely using carbon atoms. A graphene nanoribbon (GNR) is sandwiched in between diamonds, where the GNR and diamond act as a conducting wire and heat sinks, respectively, and they are smoothly connected via covalent bonds. Figure 1 shows the geometric structure of graphene-diamond hybrid structure in which the zigzag

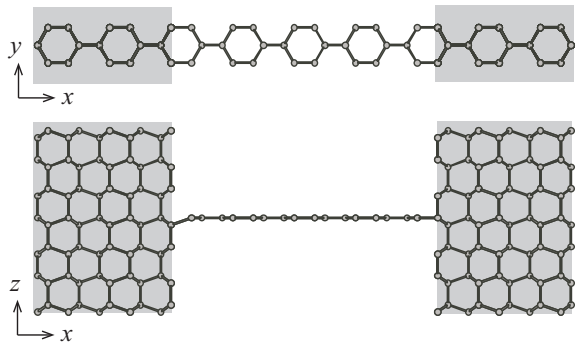

FIG. 1. Top and side views of graphene-diamond hybrid structures. The shaded area denotes the diamond region.

[a)] sokada@comas.frsc.tsukuba.ac.jp

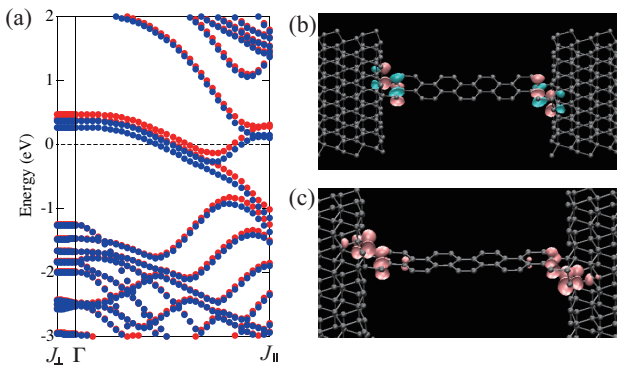

FIG. 2. (a) Electronic energy band for the high-spin state of the graphene-diamond hybrid system. Energies are measured from that of the Fermi level. Blue and red circles denote the energy dispersion for majority and minority spins, respectively. (b) Distribution of the wavefunction at $J_\parallel$ point just above the Fermi level. Color corresponds to the sign of the wave function. (c) Spin density ($\Delta\rho(\boldsymbol{r}) = \rho_{\rm up}(\boldsymbol{r}) - \rho_{\rm down}(\boldsymbol{r})$) for the high-spin state of the graphene-diamond hybrid system.

GNR is connected to the (2110) surface of the hexagonal diamonds at the both edges.

Figure 2(a) shows the electronic energy band for the high-spin state of the fully optimized hybrid structure obtained by performing the first-principles total-energy calculations based on the density functional theory[12,13]. In the calculations, we use the local spin density approximation (LSDA)[14,15] and a norm-conserving pseudopotential[16,17]. The valence wave functions are expanded by the plane-wave basis set with a cutoff energy of 50 Ry, which gives enough convergence of relative total energies and electronic structures of carbon-related materials[18,19].

As is shown in Fig. 2(a), the hybrid structure exhibits a metallic state with highly anisotropic dispersion relation. The blue and red circles denote electronic states of α-spin (majority spin) and β-spin (minority spin) states, respectively. Along the direction parallel to the ribbon (y-direction depicted in Fig. 1), most of the lectern state possess substantial dispersion of a few eV, while the states show completely flat dispersion relation in the direction normal to the ribbon (x-direction depicted in Fig. 1). Thus, as far as the electronic states around the Fermi level, the hybrid structure exhibits one-dimensional metallic nature, although the GNR is perfectly connected with the sidewalls of the diamond without any unsaturated covalent bonds. This nature is ascribed to the absence of the π electrons in the diamond region. The sp^3 carbon atoms in the diamond effectively terminate the π network associated with the graphitic network in the hybrid structure. Therefore, the hybrid structure is the possible candidates for the nanoscale conducting wire. In addition, the graphene is known to have large allowable current density ($\sim 10^9$A/cm), which is much larger than that of the copper ($\sim 10^6$A/cm). Thus, the hybrid structure can substitute the copper wire in the current semiconductor technology.

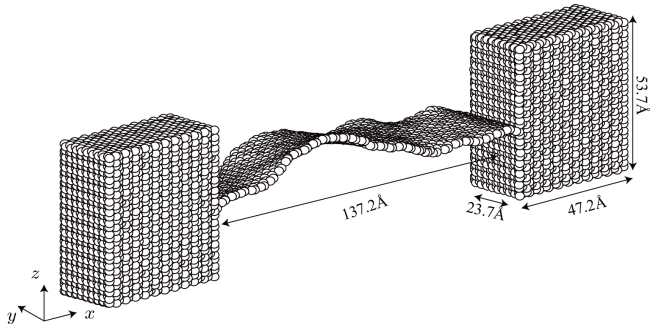

FIG. 3. MD simulation system of graphene-diamond hybrid structure.

Another fascinating property is expected in spins associated with the topological structure of the GNR region in the hybrid structure. Along the GNR, at the Fermi level, two states exhibit an unusual feature. These states exhibit flat band nature around the zone boundary and split into the energy bands for α-spin and β-spin states. Figure 2(c) corroborates that the GNR region of the hybrid structure exhibits ferromagnetic spin order. The calculated magnetic moment is 0.1 $\mu_{\rm B}$/Å, where $\mu_{\rm B}$ is the Bohr magneton. The polarized electron spin is found to be distributed around the edges of the GNR region, where the three-fold coordinated carbon atoms form zigzag border with the four-fold coordinated carbon atoms in the diamond region. By the analogies with the spin polarization on the GNR with zigzag edges[20–22], the spin polarization is associated with the edge states that have the salient characteristics in the bipartite network with particular surfaces/edges. Indeed, the distribution of the wave-function associated with the flat dispersion band corroborates their edge state nature (Fig. 2(b)). The manifestation of the spin polarization suggests that the hybrid structure can function as a spin-dependent conducting wire for nanoscale electronic device circuits.

Next, we investigate the heat-dissipation from graphene to diamond using non-equilibrium molecular dynamics (NEMD) simulations. Figure 3 shows the simulated system: a graphene sandwiched by two diamonds, which consists of 23,328 carbon atoms in total. The size of this hybrid structure is denoted in Fig. 3. The covalent bonding between carbon atoms is expressed by Tersoff-Brenner potential with the second parameter set[23–25]. After equilibration at the target temperature T for 3 ns, thermal boundary conductance between graphene and diamond was calculated by NEMD simulations. We used the velocity Verlet method for the integration of the equation of motion, and the time step Δt is set as 0.5 fs in all the simulations. A temperature gradient was applied across the system by controlling the temperature of the left and right end regions of the system at $T_{\rm H} = T + 10$ K and $T_{\rm C} = T - 10$ K, respectively. Throughout the sim-

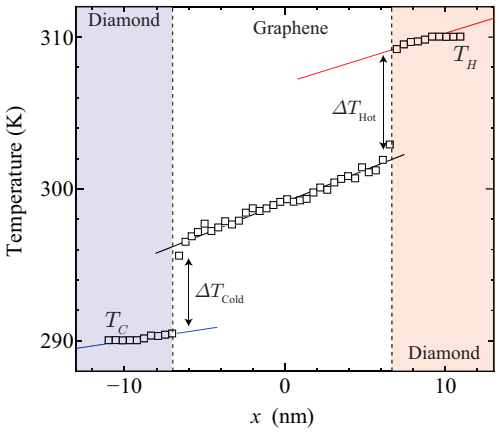

FIG. 4. Temperature profile of the graphene-diamond hybrid structure. Temperatures at hot and cold region ($T_{\rm H}$ and $T_{\rm C}$) were set as 310 and 290 K, respectively. The vertical dashed lines indicate the positions of the graphine-diamond interfaces.

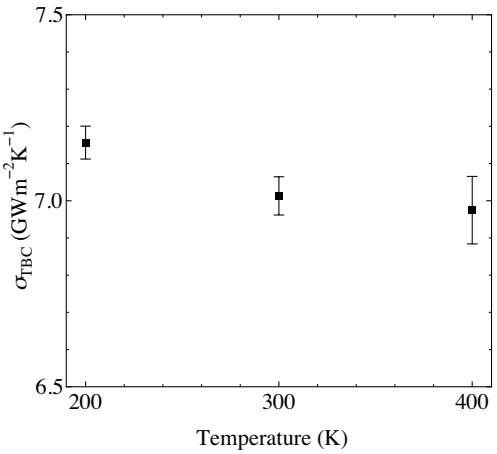

FIG. 5. Temperature dependence of the thermal boundary conductance (TBC). The $\sigma_{\rm TBC}$ is the average TBC value at the two interfaces.

ulation, the outermost diamond layers were fixed, and the temperature control was done by applying the Nosé-Hoover (NH) thermostat[26,27] to five diamond layers adjacent to the fixed end layer on each side. The relaxation parameter of NH thermostat is set as 40 fs[10] and the data are sampled for 6 ns. Heat current through this hybrid structure in the x-direction was calculated by

$$J_{\rm th} = \frac{\sum_{j=1}^{N}[\Delta Q_{\rm H}(j) - \Delta Q_{\rm C}(j)]}{2N\Delta t} \qquad (1)$$

where $\Delta Q_{\rm H/C}(j)$ denotes the added/removed kinetic energy at jth steps[28]. N is the number of NEMD simulation steps, and the factor 2 in denominator in Eq. (1) indicates the arithmetic average.

Figure 4 shows the temperature profile of the hybrid structure after the system reached steady-state with $T = 300$ K. The thermal boundary conductance, $\sigma_{\rm TBC}$, at the graphene-diamond interface can be computed as $\sigma_{\rm TBC} = J_{\rm th}/S\Delta T_{\rm ave}$, $\Delta T_{\rm ave} = (\Delta T_{\rm hot} + \Delta T_{\rm cold})/2$, where $\Delta T_{\rm hot}$ and $\Delta T_{\rm cold}$ are the temperature jumps at the interfaces on hot and cold sides, respectively (Fig. 4). S is the cross-sectional area and defined as $S = L_y \times t_g$ using interlayer distance of graphite ($t_g = 3.4$Å). As shown in Fig. 5, the obtained thermal boundary conductance exhibits weak dependence on temperature. The value of $\sigma_{\rm TBC}$ at $T = 300$ K is 7.01 ± 0.05 GWm^{-2}K^{-1}, much larger than the reported value for covalently bonded interface between carbon nanotube and silicon at $T = 300$ K (~ 0.5 GWm^{-2}K^{-1})[29] despite the similar strength and number density of the covalent bonds (0.112 and 0.083 bond/Å^{-2} for current work and Ref.[29], respectively). One possible reason for this is that the current all-carbon-atom system results in smaller frequency-mismatch between the two materials forming the interface, which is known to be a source of thermal boundary resistance[29].

In summary, we have numerically investigated the electronic, magnetic, and thermal properties of a graphene-diamond hybrid structure consisting of a graphene nanoribbon with zigzag edges covalently bonded to the diamond surfaces. The energetics as well as the electronic and magnetic states of the hybrid structure were simulated by the first-principles calculation, and their thermal transport properties were calculated by the non-equilibrium molecular-dynamics (NEMD) method. From the first-principles calculation, we found that the hybrid structure is stable and that the ferro-magnetically-ordered edge state appears around the graphene-diamond interfaces. Moreover, from the NEMD simulations, we found that the heat dissipates efficiently from the graphene to the diamond. Thus we propose that the hybrid structure is a potential candidate for spin-polarized conducting wires in the nanoscale electronic device circuits.

ACKNOWLEDGMENTS

This work was supported by the Japan Science and Technology Agency CREST and a Grant-in-Aid for Scientific Research from the Ministry of Education, Culture, Sports, Science and Technology (MEXT) of Japan.

[1] International Technology Roadmap for Semiconductors, 2011 edition.
[2] K. S. Novoselov, A. K. Geim, S. V. Morozov, D. Jiang, Y Zhang, S. V. Dubonos, I. V. Grigorieva, and A. A. Frisov, Science **306**, 666 (2004).
[3] K. S. Novoselov, A. K. Geim, S. V. Morozov, D. Jiang, M. I. Katsnelson, I. V. Grigorieva, S. V. Dubonos, and A. A. Frisov, Nature **438**, 197 (2005).
[4] K. I. Bolotin, K. J. Sikes, J. Hone, H. L. Stormer, and P. Kim, Phys. Rev. Lett. **101**, 096802 (2008).
[5] X. Du, I. Skachko, A. Barker, and E. Y. Andrei, Nature Nanotech. **3**, 491 (2008).

[6] A. A. Balandin, S. Ghosh, W. Bao, I. Calizo, D. Teweldebrhan, F. Miao, and C. N. Lau, Nano Lett. **8**, 902 (2008).
[7] P. Kim, L. Shi, A. Majumdar, and P. L. McEuen, Phys. Rev. Lett. **87**, 215502 (2001).
[8] M. Fujii, X. Zhang, H. Xie, H. Ago, K. Takahashi, T. Ikuta, H. Abe, and T. Shimizu, Phys. Rev. Lett. **95**, 065502 (2005).
[9] E. Pop, D. Mann, Q. Wang, K. Goodson, and H. Dai, Nano Lett. **6**, 96 (2006).
[10] J. Shiomi and S. Maruyama, Jpn. J. Appl. Phys. **47**, 2005 (2008).
[11] T. Yamamoto, S. Konabe, J. Shiomi and S. Maruyama, Appl. Phys. Exp. **2**, 095003 (2009).
[12] P. Hohenberg and W. Kohn, Phys. Rev. **136**, B864 (1964).
[13] W. Kohn and L. J. Sham, Phys. Rev. **140**, A1133 (1965).
[14] D. M. Ceperley and B. J. Alder, Phys. Rev. Lett. **45**, 566 (1980).
[15] J. P. Perdew and A. Zunger, Phys. Rev. B **23**, 5048 (1981).
[16] N. Troullier and J. L. Martins, Phys. Rev. B **43**, 1993 (1991).
[17] L. Kleinman and D. M. Bylander, Phys. Rev. Lett. **48**, 1425 (1982).
[18] S. Okada, S. Saito, and A. Oshiyama, Phys. Rev. Lett., **86**, 3835 (2001).
[19] S. Okada and A. Oshiyama, Phys. Rev. Lett. **87**, 146803 (2003).
[20] M. Fujita, K. Wakabayashi, K. Nakada, and K. Kusakabe, J. Phys. Soc. Jpn. **65**, 1920 (1996).
[21] K. Wakabayashi, M. Fujita, H. Ajiki, and M. Sigrist, Phys. Rev. B **59**, 8271 (1999).
[22] K. Nakada, M. Fujita, G. Dresselhaus, and M. S. Dresselhaus, Phys. Rev. B **54**, 17954 (1996).
[23] J. Tersoff, Phys. Rev. B **37**, 6991 (1988).
[24] D. W. Brenner, Phys. Rev. B **42**, 9458 (1990).
[25] D. W. Brenner, Phys. Rev. B **46**, 1948 (1992).
[26] S. Nosé, J. Chem. Phys. **81**, 511 (1984).
[27] W. G. Hoover, Phys. Rev. A **31**, 511 (1985).
[28] N. Kondo, T. Yamamoto, and K. Watanabe, e-J. Surf. Sci. Nanotech. **4**, 239 (2006).
[29] M. Hu, P. Keblinski, J. S. Wang, and N. Raravikar, J. Appl. Phys. **104**, 083503 (2008).